The Atomic Nucleus

A.-M. Mårtensson-Pendrill and M.G.H. Gustavsson

Volume 1, Part 6, Chapter 30, pp 477–484

in

Handbook of Molecular Physics and Quantum Chemistry
(ISBN 0 471 62374 1)

Edited by

Stephen Wilson

Chapter 30
The Atomic Nucleus

A.-M. Mårtensson-Pendrill[1] and M.G.H. Gustavsson[1,2]

[1] *Göteborg University and Chalmers University of Technology, Göteborg, Sweden*
[2] *Ericsson Microwave Systems AB, Sensors and Information Networks, Mölndal, Sweden*

1 INTRODUCTION

As molecules and heavy atoms are invoked for studies of fundamental interactions and properties, the demand for more accurate descriptions of the wave function within and close to the nucleus grows more stringent. With the generally increasing precision of quantum chemistry calculations, the simple point nucleus approximation resulting in the well-known Z/r potential is no longer completely adequate. The inadequacy becomes more and more evident as quantum chemistry takes on the challenge of molecules including heavy, or even super-heavy, atoms: For large Z, the behaviour close to the nucleus becomes too singular for a point-nuclear charge, and for the – still hypothetical – case of $Z > 137$, the Dirac equation breaks down. For finite nuclear distributions, the possible range extends much further.

Many properties depend on details of the nuclear structure. What are the alternatives for the nuclear distributions used in calculations? What are their advantages and disadvantages from a computational point of view? How should calculated results be presented in order to make possible meaningful comparisons between results obtained using different approaches? How much is known experimentally and how is that information best included in the calculations? These are a few of the questions addressed in this chapter.

This chapter focuses mainly on the distribution of charge, which, however, also influences other properties. In Section 4, we give a brief discussion of physical effects close to the nucleus.

Handbook of Molecular Physics and Quantum Chemistry, Edited by Stephen Wilson. Volume 1: *Fundamentals*.

ISBN: 0-471-62374-1.

2 NUCLEAR CHARGE DISTRIBUTIONS

The early theorists, without access to computers, had strong reasons to use analytical descriptions of charge distributions and potentials, which enabled series expansions of analytical solutions of the wave functions within and close to the nucleus. A common choice was the homogeneous charge distribution inside a radius $R = R_0 A^{1/3}$, where A is the mass number of the nucleus. The most important parameter for many properties is the expectation value $\langle r^2 \rangle$, which has the value $3R^2/5$ for the homogeneous nucleus. This simple distribution gives the correct analytical behaviour of the electronic wave functions at $r = 0$ and has been used in many early analyses and is discussed in more detail in Section 3.2. These expansions are also useful for a general understanding of the effects involved.

2.1 Experimental information

Experimental information about charge distributions is derived from many sources, including electron scattering. The experimental data indicate that $R_0 \simeq 1.2\,\text{fm}$

gives a reasonable approximation for the homogeneous distribution. Clearly, the tail of a real nucleus is less sharp than indicated by the homogeneous distributions. It is often described in terms of a 'skin thickness' t, defined as the distance in which the charge density falls from 90% of its central value to 10%. Experiments indicate that t is about 2.3 fm for most nuclei.

The primary data from electron-scattering experiments are expressed in terms of a 'Fourier–Bessel expansion'. Figure 1 shows the resulting charge distribution for several different nuclei. It is possible to use these data directly using a numerical approach, as shown in Section 3.1. Tabulations often give values relating to additional parameterizations, in particular, the two and three-parameter Fermi distributions as well as the Gaussian expansions,[1,2] that are discussed in more detail in the following text.

Another source are muonic X-ray energies. These probe somewhat different moments, the 'Barrett moments' $\langle r^k e^{-\alpha r}\rangle$, of the nuclear distribution. Nevertheless, the results are quoted also in terms of $\langle r^2\rangle$.[3]

Optical isotope shifts provide an important source of complementary information, particularly for chains of radioactive isotopes. It is found that the changes in charge radius along an isotope chain are, in general, smaller than those indicated by the aforementioned textbook formula. The isotope shifts also reveal an 'odd–even staggering' of the $\langle r^2\rangle$ values, providing evidence of nuclear shell structure.[4,5] A spectacular recent application is the precision determination of the 'deuteron structure radius' from the hydrogen-deuterium isotope shift of the 1s–2s two-photon resonance.[6]

2.2 Nuclear distributions and electronic wave functions

The electrostatic potential energy, $V(r)$, for an electron in a spherically symmetric charge distribution, $\rho(r)$, is given by the well-known expression

$$V(r) = -\frac{e}{4\pi\epsilon_0}\left[\frac{4\pi}{r}\int_0^r \rho(r')r'^2\,\mathrm{d}r' + 4\pi\int_r^\infty \frac{1}{r'}\rho(r')r'^2\,\mathrm{d}r'\right]$$

Outside the nucleus, this expression reduces to the same potential, $-Ze^2/4\pi\epsilon_0 r$, as from a point nucleus. For a

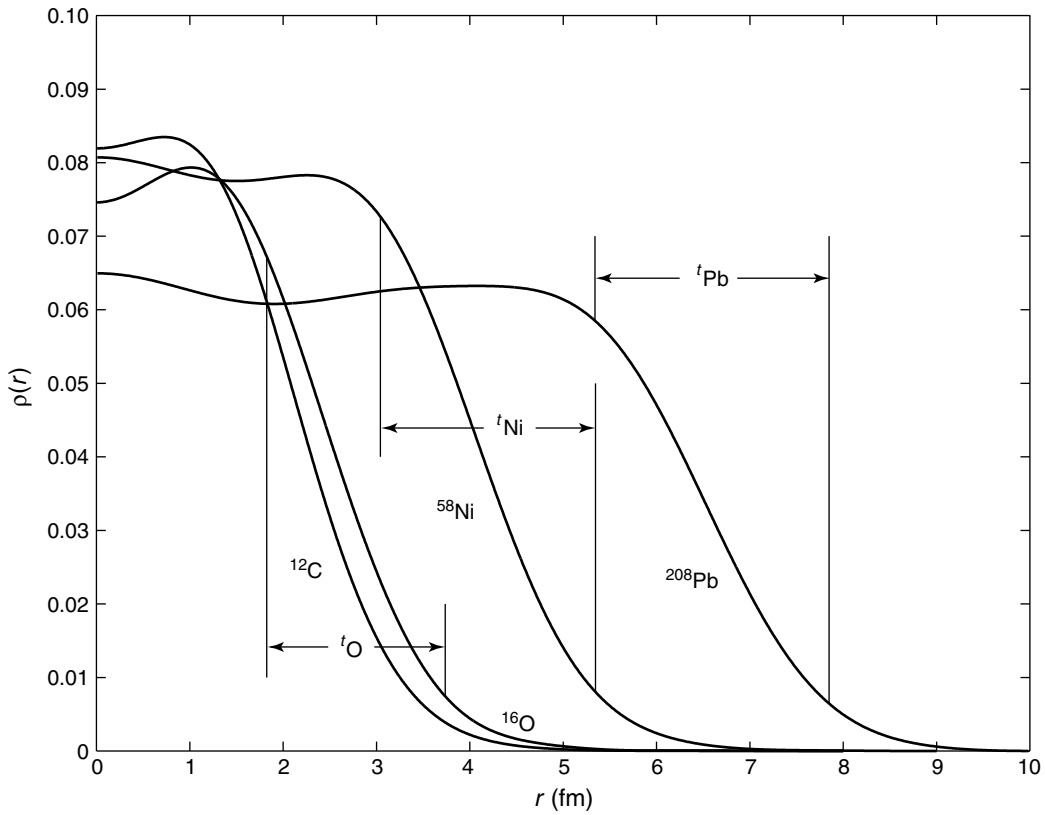

Figure 1. The radial charge distribution for several nuclei determined by electron scattering. The skin thickness t is shown for O, Ni, and Pb; its value is roughly constant at 2.3 fm. These distributions were obtained from Fourier–Bessel expansion data tabulated by de Vries, H., de Jager, C.W., and de Vries, C. (1987).[1]

homogeneous distribution, where $\rho(r) = 3Ze/4\pi R^3$ within a nuclear radius R, the electrostatic potential for $r \leq R$ is

$$V(r) = -\frac{1}{4\pi\epsilon_0}\frac{Ze^2}{r}\left(\frac{3r}{2R} - \frac{r^3}{2R^3}\right) \tag{1}$$

We note that the potential is essentially constant at $V_0 = -(1/4\pi\epsilon_0) \times (3Ze^2/2R)$ very close to the origin. This determines the behaviour of the orbitals for very small r, which is obtained by a series expansion of the coupled radial equations from the Dirac equation:

$$\begin{aligned} -\hbar c\left[\frac{\mathrm{d}}{\mathrm{d}r} - \frac{\kappa}{r}\right] G(r) &= [\varepsilon - V(r)]\, F(r) \\ \hbar c\left[\frac{\mathrm{d}}{\mathrm{d}r} + \frac{\kappa}{r}\right] F(r) &= \left[\varepsilon + 2m_e c^2 - V(r)\right] G(r) \end{aligned} \tag{2}$$

where $\kappa = \mp(j + 1/2)$ for $j = l \pm 1/2$, ε is the binding energy, and $F(r)$ and $G(r)$ are the radial parts of the 'large' and 'small' components, respectively, of a relativistic wave function. (The sign relation in equation (2) between F and G is valid for the 'ls-convention' for the coupling of spin and orbital angular momentum.)

In the following text, we use atomic units, where $e = m_e = 4\pi\epsilon_0 = \hbar = 1$ and $c = 1/\alpha \approx 137$. (A word of caution: Relativistic atomic calculations form a meeting ground between traditional atomic and molecular calculations and field theoretical approaches, where the equations are instead expressed in 'natural units', where $c = m_e = 4\pi\epsilon_0 = \hbar = 1$ and $e^2 = \alpha \approx 1/137$).

For a point nucleus, the leading term is r^γ, where $\gamma = \sqrt{[\kappa^2 - (Z\alpha)^2]}$ for both $F(r)$ and $G(r)$. The solution $r^{-\gamma}$ is singular for $r = 0$ and must be rejected for point nuclei. For an extended nucleus, however, this term enters with a small coefficient in the matching of outer and inner solutions.

Inside an extended nucleus, the leading term in the upper component is r^l. For $j = l + 1/2$ orbitals, the lower component carries an extra factor r, whereas for $j = l - 1/2$ orbitals, the lower component has a small term r^{l-1} that dominates for very small r.

We note that atomic orbitals with $j = 1/2$ (i.e., s and $p_{1/2}$) have an appreciable probability within the nucleus, where their density is essentially constant. The effect

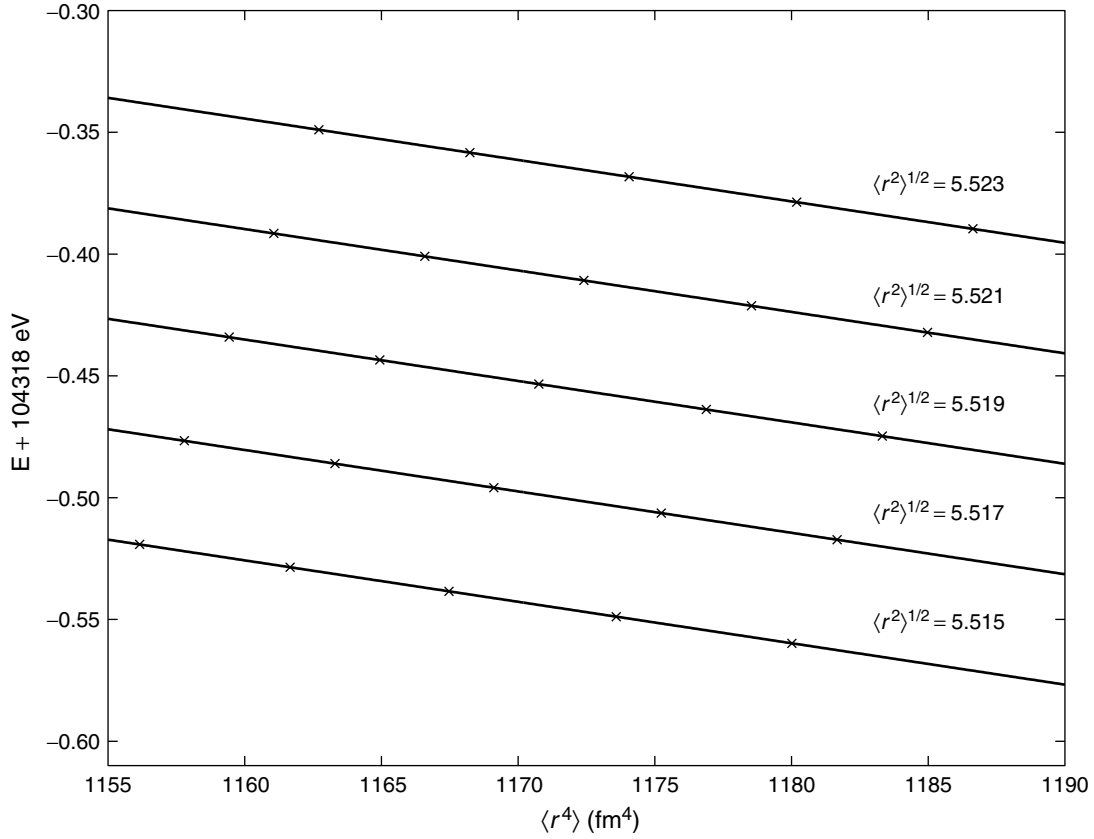

Figure 2. The dependence of the ground state energy of hydrogen-like bismuth on the nuclear charge distribution. The lines show results for constant values of the nuclear root-mean-square (rms) radius and were obtained by fitting a linear expansion in $\langle r^4 \rangle$ to the results of explicit numerical calculations (marked by crosses) for different values of the nuclear parameters.

of the nuclear distribution on atomic properties then becomes proportional to the expectation value, $\langle r^2 \rangle = \int r^2 \rho(\boldsymbol{r})\, \mathrm{d}V / \int \rho(\boldsymbol{r})\, \mathrm{d}V$, of the nuclear distribution. This observation is well known from studies of optical isotope shifts, which are changes in transition frequency between different isotopes of an element. The 'field' or 'volume' isotope shift is the part due to the different charge distributions and is expressed as $\delta\nu = F\delta\langle r^2 \rangle$, where $F = (2\pi/3)(Ze^2/4\pi\epsilon_0)\Delta|\Psi(0)|^2$.

For heavy nuclei, the next terms in the expansion of the wave functions also become significant. Thus, higher moments $\delta\langle r^4 \rangle$, $\delta\langle r^6 \rangle, \ldots$ of the nuclear distribution also contribute. As an illustration, Figure 2, shows the 1s energy for hydrogen-like Bi ($Z = 83$) for Fermi distributions with various values of $\langle r^2 \rangle$ and $\langle r^4 \rangle$.

The electron density then varies within the nucleus, giving contributions from higher moments. These 'Seltzer corrections'[7] can be accounted for by including a factor κ, which is, for example, about 0.92 for Bi.[8] These factors are of course not needed if the distribution is included directly in the calculation.

In the following text, we consider in more detail the expression for potentials and orbitals for homogeneous, Fermi, and Gaussian models of the nuclear distributions. Several other distributions have been considered in detail by Andrae,[9] who provides expressions for wave functions and energy corrections for a wide range of nuclear distributions as well as a comparison of first-order energy corrections for one-electron systems with exact ones for nonrelativistic and relativistic treatments.

3 FINITE NUCLEAR CHARGE DISTRIBUTIONS

In this section, we give a brief presentation of models commonly used to account for the experimentally obtained information about the nuclear distribution. We also present the resulting potential and discuss the related initial conditions and orbital behaviour for small r values.

3.1 Electron scattering and the Fourier–Bessel expansion

The data from electron scattering are analysed using the Plane Wave Born Approximation, and the charge distribution is obtained as the Fourier transform of the form factors $F(q)$, giving for a spherically symmetric charge distribution

$$\rho(r) = \frac{1}{2\pi^2} \int F(q) \frac{\sin(qr)}{qr} q^2\, \mathrm{d}q$$

The accuracy is limited by the finite range of q values. The Fourier–Bessel analysis, introduced by Dreher and co-workers,[10] assumes a cut-off radius for the nucleus and uses an analytical approximation for the form factor $F(q)$ for q values beyond the maximum available value. The charge distribution is then written as

$$\rho(r) = \begin{cases} \sum_\nu a_\nu j_0\left(\dfrac{\nu\pi r}{R}\right) & \text{for } r \le R \\ 0 & \text{for } r > R \end{cases}$$

where $j_0(x) = \sin(x)/x$ is the zeroth-order spherical Bessel function. The first few coefficients are deduced from experiments and are given in tabulations.[1,2]

The expressions for the total charge Q and the potential energy $V(r)$ are

$$Q = 4\pi \sum_\nu a_\nu \left(\frac{R}{\nu\pi}\right)^3 \nu\pi(-1)^{\nu+1}$$

$$V(r) = \begin{cases} -4\pi \sum_\nu a_\nu \left(\dfrac{R}{\nu\pi}\right)^2 \left[j_0\left(\dfrac{\nu\pi r}{R}\right) - (-1)^\nu \right] & \text{for } r \le R \\ -\dfrac{Z}{r} & \text{for } r > R \end{cases}$$

This potential has been applied in the case of the ground state hyperfine structure (hfs) of hydrogen-like Bi.[11]

The second moment, $\langle r^2 \rangle$, of the charge distribution can also be expressed in terms of the Fourier–Bessel parameters:

$$\langle r^2 \rangle = \frac{4\pi}{Q} \sum_\nu a_\nu \left(\frac{R}{\nu\pi}\right)^5 \nu\pi(-1)^\nu \left[6 - (\nu\pi)^2\right]$$

and is usually quoted in tabulations as well as values for the Fermi and Gaussian parametrizations, which are discussed later.

3.2 Uniform distribution and orbital expansions

The uniform distribution of charge within a radius R was discussed briefly in Section 2.2. Obviously, there is a discontinuity in the charge distribution, $\rho(r)$, at the nuclear boundary, leading to a discontinuity in the second derivative of the potential at $r = R$. Care must thus be taken in numerical integration schemes to avoid spurious effects related to the nuclear boundary. In numerical approaches, the discontinuity also leads to slower convergence with the grid spacing.[12]

To find a detailed description for the orbital behaviour for very small r, a power series Ansatz for the orbitals

is inserted together with the expression for the potential equation (1) in the radial Dirac equation (2).

To facilitate the notation in the orbital expansion, we write the potential in the form $V(r, R) = V_0 + V_2 r^2$, where $V_0 = -3Z/2R$ and $V_2 = -V_0/3R^2$ for the homogeneous distribution. The other potentials discussed in the following text lead, in addition, to terms of the type $V_3 r^3$ and higher, which affect the higher-order terms in the series expansion of the orbitals. Using these parameters and the binding energy ϵ and keeping the lowest-order terms gives for $\kappa < 0$

$$F(r) = N\left\{r^{|\kappa|} - \frac{(\varepsilon - V_0)(\varepsilon + 2c^2 + V_0)}{2c^2(1 + 2|\kappa|)} r^{|\kappa|+2} \dots\right\}$$

$$G(r) = N\left\{-\frac{\varepsilon - V_0}{c(1 + 2|\kappa|)} r^{|\kappa|+1} + \left[\frac{(\varepsilon - V_0)^2(\varepsilon + 2c^2 + V_0)}{2c^3(1 + 2|\kappa|)(3 + 2|\kappa|)} + \frac{V_2}{c(3 + 2|\kappa|)}\right] r^{|\kappa|+3} \dots\right\}$$

and for $\kappa > 0$

$$F(r) = N\left\{r^{\kappa+1} - \left[\frac{(\varepsilon - V_0)(\varepsilon + 2c^2 - V_0)}{2c^2(3 + 2\kappa)} + \frac{V_2(1 + 2\kappa)}{(\varepsilon + 2c^2 - V_0)(3 + 2\kappa)}\right] r^{\kappa+3} \dots\right\}$$

$$G(r) = N\left\{\frac{c(1 + 2\kappa)}{\varepsilon + 2c^2 - V_0} r^{\kappa} - \frac{\varepsilon - V_0}{2c} r^{\kappa+2} \dots\right\}$$

where N is a normalizing constant.

The energy dependence of these expressions is very weak, since the binding energy ε is much smaller than the potential energy $V_0 = -3Z/2R$ at $r = 0$, particularly for low Z.

3.3 Fermi distribution

The two-parameter Fermi model gives a realistic description of the nuclear distribution,[13,14] and at the same time provides considerable flexibility in the analysis:

$$\rho(r) = \frac{\rho_0}{1 + e^{(r-c)/a}} \tag{3}$$

where c is the half-density radius and a is related to the skin thickness t by $t = (4 \ln 3)a$, giving values of a that is roughly constant at 0.524 fm. For vanishing skin thickness, the Fermi form reduces to the homogeneous distribution with a radius $R = c$.

The shape of the Fermi distribution is identical to that of the Woods–Saxon potential. The analogy between the nuclear distribution and potential is related to the short-range character of the strong interaction, which holds the nucleus together.

The shape of an arbitrary nuclear distribution can often be adequately described by the moments $\langle r^{2n} \rangle$ of the distribution. Varying the parameter in the Fermi distribution makes it possible to study the influence of the higher nuclear moments, $\langle r^{2n} \rangle$, given to a good approximation,[11] by the relations

$$\langle r^2 \rangle \approx \frac{3}{5}c^2 + \frac{7}{5}\pi^2 a^2$$

$$\langle r^4 \rangle \approx \frac{3}{7}c^4 + \frac{18}{7}\pi^2 a^2 c^2 + \frac{31}{7}\pi^4 a^4$$

$$\langle r^6 \rangle \approx \frac{3}{9}c^6 + \frac{11}{3}\pi^2 a^2 c^4 + \frac{239}{15}\pi^4 a^4 c^2 + \frac{127}{5}\pi^6 a^6$$

The electrostatic potential cannot be obtained analytically for the Fermi distribution equation (3). However, convenient expressions for the evaluation of the potential have been derived[15] and are used in the procedure adopted in the general atomic structure package of computer programs GRASP[2],[16,17] and are summarized briefly in the following text.

The radial integrals can be written in terms of infinite series, which converge to machine precision with just a few terms included. The potential energy for $r < c$ can be written as

$$V_{r<c}(r) = -\frac{N}{r}\left[\frac{3r}{2c} - \frac{r^3}{2c^3} + \frac{r\pi^2 a^2}{2c^3} - \frac{3ra^2}{c^3} S_2\left(\frac{r-c}{a}\right) + \frac{6a^3}{c^3} S_3\left(\frac{r-c}{a}\right) - \frac{6a^3}{c^3} S_3\left(-\frac{c}{a}\right)\right]$$

and for the case $r > c$, we have

$$V_{r>c}(r) = -\frac{N}{r}\left[1 + \frac{\pi^2 a^2}{c^2} + \frac{3ra^2}{c^3} S_2\left(-\frac{r-c}{a}\right) + \frac{6a^3}{c^3} S_3\left(-\frac{r-c}{a}\right) - \frac{6a^3}{c^3} S_3\left(-\frac{c}{a}\right)\right]$$

where the S_k functions are given by

$$S_k(x) = \sum_{n=1}^{\infty} (-1)^n \frac{e^{xn}}{n^k}$$

and the normalization condition gives

$$N = \frac{Z}{\left[1 + \frac{\pi^2 a^2}{c^2} - \frac{6a^3}{c^3} S_3\left(-\frac{c}{a}\right)\right]}$$

In the expression for the potential within the nucleus, we recognize the constant term $V_0 = -3Z/2c$ from the uniform distribution for the case of vanishing skin thickness.

3.3.1 Deformed nuclei

Generalizations of the Fermi model to describe deformed nuclei have been applied, for example, in the study of energies for highly charged uranium.[18,19] The nuclear radius parameter c in the Fermi distribution equation (3) is then replaced by

$$R(\boldsymbol{r}) = c\left[1 + \beta_2 Y_{20}(\boldsymbol{r}) + \beta_4 Y_{40}(\boldsymbol{r})\right] \tag{4}$$

which includes an explicit dependence on the angular coordinates.

3.3.2 The three-parameter Fermi model

The three-parameter Fermi distribution makes it possible to reproduce the small dip found in the charge distribution for small r, as seen in Figure 1.

3.4 Gaussian expansions

Many quantum chemistry programs expand the electronic wave functions in terms of Gaussian-type functions. Using a Gaussian charge distribution then has the advantage of making it possible to evaluate electron–nucleus interactions using the same integral routines as the electron–electron interactions. Visscher and Dyall[12] in their comparison of different approaches use a one-parameter Gaussian distribution $\rho(r) = Z\,(\xi/\pi)^{3/2}\exp(-\xi r^2)$ where the width is determined from the experimental rms radius $\xi = 3/\langle 2r^2\rangle$, giving a potential related to the error function $V(r) = -(Z/r) \times \mathrm{erf}[(\sqrt{\xi})r]$. Visscher and Dyall[12] found that this one-parameter Gaussian potential reproduced about 99% of the correction to the energies for high Z, whereas the uniform distribution gave about 100.1% of the correction, indicating the importance of the higher $\langle r^{2n}\rangle$ moments.

In order to obtain a model-independent fit of the charge distribution, a parametrization of the experimental data into a sum of Gaussians was suggested by Sick.[20] The width γ of the Gaussians is chosen to be equal to the smallest width of the peaks in the nuclear radial wave functions calculated by the Hartree–Fock method. Only positive values of the amplitudes of the Gaussians are allowed so that no structures narrower than γ can be created through interference. An advantage of the use of Gaussians is that values of $\rho(r)$ at different values of r are decoupled to a large extent because of the rapid decrease of the Gaussian tail. The charge distribution is then expressed as

$$\rho(r) = \sum_i A_i \left\{ \mathrm{e}^{-[(r-R_i)/\gamma]^2} + \mathrm{e}^{-[(r+R_i)/\gamma]^2} \right\}$$

where the coefficients A_i are given by

$$A_i = \frac{ZeQ_i}{2\pi^{3/2}\gamma^3\left(1 + 2R_i^2/\gamma^2\right)}$$

In this definition, the values of Q_i indicate the fraction of the charge contained in the ith Gaussian, normalized such that

$$\sum_i Q_i = 1$$

The second term for each parameter, centred around a nonphysical negative R_i value, is included to ensure that the slope of the distribution is indentically zero at the origin. An additional advantage over the Fourier–Bessel expansion is that the sum-over Gaussians by construction can give only nonnegative values for $\rho(r)$.

The relevant parameters can be found tabulated, as in the case of the Fourier–Bessel expansion.[1,2] For high-spin nuclei, it might be valuable to include an angular dependence in analogy with equation (4). In general, they give a better description of the inner part of the nucleus better than the Fourier–Bessel expansion, which, on the other hand, gives a better description in the outer part where the Gaussian tail decays too rapidly. Since an electronic wave function is more sensitive to the outer part of the nuclear distribution, the Fourier–Bessel expansion is preferable. On the other hand, the main part of the energy correction (which in itself is only 0.12% for $Z = 100$) is accounted for already with the one-parameter Gaussian potential, so the Gaussian expansion should clearly be adequate for most applications.

4 PHYSICS NEAR THE NUCLEUS

The energy of a system is only weakly influenced by details in the nuclear charge distribution. Even for $Z = 100$, using an extended nuclear charge gives only an 0.1% reduction of the binding energy. Differences between different distributions are less than a percent of the correction itself. However, several atomic properties depend directly on the wave function close to the nucleus. Using a point charge, with the resulting unphysical behaviour of the wave function at $r = 0$ then leads to overestimates by several percent for high Z.

An important observation in the study of nuclear properties is that the orbital behaviour within the nucleus

depends on the angular momentum but is essentially independent of the binding energy. For very heavy nuclei, the binding energies are a larger fraction of the nuclear potential energy, giving a small n-dependence in the orbital behaviour close to the nucleus, as demonstrated, for example, by Shabaev[21] for hfs corrections for different values of Z.

For a many-electron system, all electrons are affected but mainly through their interaction with the modified $j = 1/2$ orbitals. It is then the sensitivity of the interaction of the $j = 1/2$ orbitals that needs to be studied in detail. A striking illustration is the comparison by Visscher and Dyall[12] of the relation between the corrections for the 1s orbital energy and the total energy. The ratio between the corrections to the point nuclear value for Fermi, homogeneous, and Gaussian distribution were plotted for both cases, giving two figures differing only in their captions. In this way, nuclear size effects obtained for one charge distribution could be rescaled to another distribution by applying correction factors determined from the effects on the s orbitals. (The difference between the higher moment contributions for s and $p_{1/2}$ is relatively insignificant.)

As discussed in previous sections, the shape can be parametrized in terms of the moment $\langle r^2 \rangle$, $\langle r^4 \rangle$, and $\langle r^6 \rangle$ of the nuclear charge. To facilitate comparisons between different calculations, we therefore suggest that whatever nuclear distribution is used, these moments should be given (or sufficient information provided to make their extraction easy).

4.1 Hyperfine structure

The best-known example of nuclear-structure effects in atomic spectra is the magnetic hfs, which arises from a coupling between the magnetic moments of the nucleus and the electron, given by

$$h_{\mathrm{p}}^{\mathrm{hfs}} = \hat{\boldsymbol{r}} \cdot \frac{\boldsymbol{\mu} \times \boldsymbol{\alpha}}{r^2}$$

for a point magnetic dipole.

The resulting energy splitting is often expressed as $A\mathbf{I}\cdot\mathbf{J}$, where $\mathbf{I}$ and $\mathbf{J}$, are the angular momenta of the nucleus and the electron, respectively. The hfs was an early source of information about nuclear spin, magnetic moments. In general, magnetic moments are known better through other sources, such as nuclear magnetic resonance (NMR). Hyperfine structure can thus be used to test atomic wave functions.[22]

The ratio between the magnetic moment and the 'A-factor' is, however, found to vary slightly between various isotopes of an element. Part of this 'hyperfine anomaly' arises from differences in the charge distribution (the so-called Breit–Rosenthal effect). Another contribution to the hyperfine anomaly, the 'Bohr–Weisskopf effect' arises from the distribution of nuclear magnetic moment. In this way, the hyperfine anomaly can give information about magnetic moment distribution.

4.2 Parity nonconserving operators

The study of parity nonconserving weak interaction has been a fruitful branch of atomic physics. Recent experiments for Cs are accurate at the percent level, providing a serious challenge to atomic theory. The electro-weak interaction involves the neutron distribution, and James and Sandars[23] have analysed in detail the sensitivity to details in the distribution. Experimental information can possibly be obtained from hyperfine anomalies, as in the recent experiments for Fr isotopes.[24]

The near-energy independence of the orbital shape close to the nucleus forms the basis for derivations of relations between different interactions close to the nucleus by using the series expansion of the wave function. The ratios are, however, modified by many-body corrections if the operators have different angular structure, as discussed, for example, in Reference 25. This has long been used to estimate field isotope shifts from observed hfs[26,4] and more recently for various P and T violating operators.[27,28,29] The 'Schiff moments', for example, involve the difference between the charge and electric dipole distributions.

5 CONCLUDING REMARKS

As quantum chemists approach systems with increasingly heavy atoms, the use of an extended charge distribution becomes essential, and the charge distribution used must be clearly specified to make possible comparison of different results.

REFERENCES

1. de Vries, H., de Jager, C.W., and de Vries, C. (1987) *Atomic Data Nucl. Data Tables*, **36**(3), 495.
2. Fricke, G., Bernhardt, C., Heilig, K., Schaller, L.A., Schellenberg, L., Schera, E.B., and de Jager, C.W. (1995) *Atomic Data Nucl. Data Tables*, **60**(2), 177.
3. Engfer, R., Schneuwly, H., Vuilleumier, J.L., Walter, H.K., and Zehnder, A. (1974) *Atomic Data Nucl. Data Tables*, **14**(5–6), 509.
4. Aufmuth, P., Heilig, K., and Steudel, A. (1987) *Atomic Data Nucl. Data Tables*, **37**(3), 455.

5. Otten, E.W. (1989) *Treatise Heavy-Ion Sci.*, **8**, 517.
6. Huber, A., Udem, T., Gross, B., Reichert, J., Kourogi, M., Pachucki, K., Weitz, M., and Hänsch, T.W. (1998) *Phys. Rev. Lett.*, **80**(3), 468.
7. Seltzer, E.C. (1969) *Phys. Rev.*, **188**(4), 1916.
8. Torbohm, G., Fricke, B., and Rosén, A. (1985) *Phys. Rev. A*, **31**(4), 2038.
9. Andrae, D. (2000) *Phys. Rep.*, **336**(6), 413.
10. Dreher, B., Friedrich, J., Merle, K., Rothhaas, H., and Lührs, G. (1974) *Nucl. Phys.*, **A235**(1), 219.
11. Gustavsson, M.G.H. and Mårtensson-Pendrill, A.-M. (1998) *Adv. Quantum Chem.*, **30**, 343.
12. Visscher, L. and Dyall, K.G. (1997) *Atomic Data Nucl. Data Tables*, **67**(2), 207.
13. Hofstadter, R., Fechter, H.R., and McIntyre, J.A. (1953) *Phys. Rev.*, **92**(4), 978.
14. Hahn, B., Ravenhall, D.G., and Hofstadter, R. (1956) *Phys. Rev.*, **101**(3), 1131.
15. Parpia, F.A. and Mohanty, A.K. (1992) *Phys. Rev. A*, **46**(7), 3735.
16. Dyall, K.G., Grant, I.P., Johnson, C.T., Parpia, F.A., and Plummer, E.P. (1989) *Comput. Phys. Commun.*, **55**(3), 425.
17. Parpia, F.A. and Grant, I.P. (1991) *J. de Physique IV*, **1** (C1), 33.
18. Indelicato, P. and Lindroth, E. (1992) *Phys. Rev. A*, **46**(5), 2426.
19. Ynnerman, A., James, J., Lindgren, I., Persson, H., and Salomonson, S. (1994) *Phys. Rev. A*, **50**(6), 4671.
20. Sick, I. (1974) *Nucl. Phys.*, **A218**(3), 509.
21. Shabaev, V.M. (1994) *J. Phys. B*, **27**(24), 5825.
22. Safronova, M.S., Johnson, W.R., and Derevianko, A. (1999) *Phys. Rev. A*, **60**(6), 4476.
23. James, J. and Sandars, P.G.H. (1999) *J. Phys. B*, **32**(14), 3295.
24. Grossman, J.S., Orozco, L.A., Pearson, M.R., Simsarian, J.E., Sprouse, G.D., and Zhao, W.Z. (1999) *Phys. Rev. Lett.*, **83**(5), 935.
25. Mårtensson-Pendrill, A.-M., Pendrill, L., Salomonson, S., Ynnerman, A., and Warston, H. (1990) *J. Phys. B*, **23**(11), 1749.
26. Kopfermann, H. (1958) *Nuclear Moments*, Academic Press, New York.
27. Sushkov, O.P., Flambaum, V.V., and Khriplovich, I.B. (1984) *Sov. Phys. – JETP*, **60**(5), 873.
28. Sushkov, O.P., Flambaum, V.V., and Khriplovich, I.B. (1984) *Zhurnal Eksperimental'noi i Teoreticheskoi Fiziki*, **87**(5), 1521.
29. Mårtensson-Pendrill, A.-M. (1992) Calculations of P- and T-Violating Properties in Atoms and Molecules, in *'Methods in Computational Chemistry'*, Vol. 5: *Atomic and Molecular Properties*, ed. S. Wilson, Plenum Press, New York, 99–156.